

STAGNATION POINT FLOW OF MHD DUSTY FLUID TOWARD STRETCHING SHEET WITH CONVECTIVE SURFACE

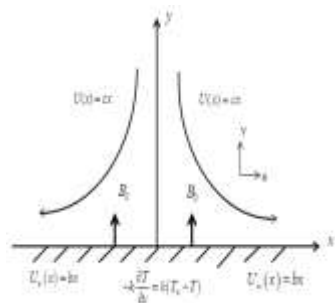
Sharena Mohamad Isa, Anati Ali*, Sharidan Shafie

Department of Mathematical Sciences, Faculty of Sciences, Universiti Teknologi Malaysia, 81310, UTM Johor Bahru, Johor, Malaysia.

Article history
Received
10 February 2015
Received in revised form
10 November 2015
Accepted
12 November 2015

*Corresponding author
anati@utm.my

Graphical abstract



Abstract

This paper presents the study of stagnation point of hydromagnetic flow of dusty fluid over a stretching sheet with the bottom surface of sheet heated by convection from hot fluid. The governing partial differential equations are transformed into a system of nonlinear ordinary differential equations using similarity transformation. These resulting nonlinear ordinary differential equations are solved numerically by using Runge-Kutta Fehlberg fourth-fifth order method (RKF45 Method). The characteristics of velocity and temperature profiles of hydromagnetic fluid flow of dusty fluid are analyzed and discussed for different parameters of interest such as convective Biot number, fluid-particle interaction parameter, magnetic parameter, ratio of free stream velocity parameter and Prandtl number on the flow. The numerical results are compared with previous published results for validation.

Keywords: Boundary layer flow; dusty fluid; stagnation point flow; convective boundary condition

Abstrak

Kertas kerja ini membentangkan kajian mengenai titik genangan pada aliran bendalir hidromagnet berdebu melalui satu lembaran regangan dipanaskan oleh olakan dari aliran panas. Persamaan pembezaan separa diturunkan kepada persamaan pembezaan biasa tak linear menggunakan penjelmaan serupa. Persamaan pembezaan biasa tak linear ini diselesaikan secara berangka dengan menggunakan kaedah Runge-Kutta Fehlberg peringkat keempat-kelima (Kaedah RKF45). Ciri-ciri profil halaju dan suhu aliran bendalir hidromagnet berdebu ini dianalisis dan dibincangkan bagi parameter yang bertalian kepentingan seperti nombor Biot olakan, parameter interaksi bendalir-zarah, parameter magnet, nisbah parameter halaju aliran bebas dan nombor Prandtl pada aliran.

Kata kunci: Aliran lapisan sempadan; aliran berdebu; aliran titik genangan; syarat sempadan olakan

© 2016 Penerbit UTM Press. All rights reserved

1.0 INTRODUCTION

In recent times, the investigation on two phase flows in which solid spherical particles are distributed in fluid

becomes extensive research in fluid dynamics which can be observed in natural phenomenon such as atmospheric flow during storm and flow of mud water in river, canal or pond. The study of dusty fluid becomes

essential due to its important in engineering applications and technical problems such as flow through packed beds, sedimentation, environmental pollution, centrifugal separation of particles and blood rheology. In view of these applications, Saffman [1] discussed the stability of the motion of a gas carrying small dust particles. Chakrabarti [2] investigated the boundary layer of dusty gas. Then, Vajravelu and Nayfeh [3] studied the hydromagnetic flow of dusty fluid over a stretching surface with the presence of suction. The study of boundary layer flow and heat transfer induced by continuous stretching surfaces becomes essential due to its wide applications in engineering problems such as polymer sheet extrusion from a dye, glass fiber and paper production, drawing of plastic films, etc. Therefore, the study of dusty fluid for different physical situations was made. [4-6]

From a technological view, the stagnation-point flow and the flow due to a stretching sheet are equally important in theoretical and also in applications. A stagnation point flow described that, fluid motion near the stagnation region exist on a solid body where the fluid moves toward it where solid body corresponds to

either fix or moving surfaces in a fluid. Chaim [7] was the first to study the steady two-dimensional stagnation-point flow towards a stretching sheet. Whereas, Bhattacharyya [8] studied the effect of non-uniform heat flux on heat transfer in boundary layer stagnation-point flow over a shrinking sheet. Then, Ramesh et al. [9] investigated stagnation point on hydromagnetic flow of dusty fluid over a permeable stretching sheet with the presence of non-uniform source/sink. Ramesh et al. [10] analyzed the effect of radiation on stagnation point flow of electrically conducting dusty fluid toward stretching surface.

The aim of the present paper is to study the hydromagnetic stagnation point flow of dusty fluid toward a stretching surface with convective boundary condition. The coupled nonlinear partial differential equations are transformed into a couple nonlinear ordinary differential equations by using similarity transformation. These nonlinear ordinary differential equations are solved numerically by using Runge Kutta Fehlberg forth-fifth order method (RK45 Method) for different values of parameters.

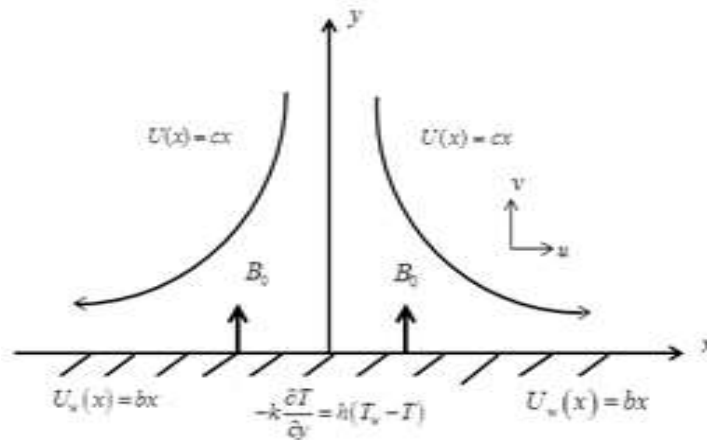


Figure 1 Schematic diagram of the two-dimensional stretching sheet

2.0 MATHEMATICAL FORMULATION

Consider a steady two dimensional laminar boundary layer flow of a viscous, incompressible and electrically conducting dusty fluid near the stagnation point flow over a stretching sheet. The flow produced by action of two equal and opposite forces along the x-axis and y-axis being normal to the flow. It is assumed that the free stream and the stretching velocities are of the forms $U(x)$ and $U_w(x)$ respectively. The dust particles are assumed to be in spherical in shape and uniform in size and number density of these are taken as a constant throughout the flow. Under these assumptions, the governing equations in the usual notation can be written as

$$\frac{\partial u}{\partial x} + \frac{\partial v}{\partial y} = 0 \tag{1}$$

$$\rho_\infty \left(u \frac{\partial u}{\partial x} + v \frac{\partial u}{\partial y} \right) = \mu \frac{\partial^2 u}{\partial y^2} + \frac{\rho_p}{\tau} (u_p - u) - \frac{dP}{dx} - \sigma_0 B_0^2 u \tag{2}$$

$$\rho_\infty C_p \left(u \frac{\partial T}{\partial x} + v \frac{\partial T}{\partial y} \right) = k \frac{\partial^2 T}{\partial y^2} + \frac{C_s \rho_p}{\gamma_T} (T_p - T) \tag{3}$$

$$\frac{\partial}{\partial x} (\rho_p u_p) + \frac{\partial}{\partial y} (\rho_p v_p) = 0 \tag{4}$$

$$u_p \frac{\partial u_p}{\partial x} + v_p \frac{\partial u_p}{\partial y} = \frac{1}{\tau} (u - u_p) \tag{5}$$

$$u_p \frac{\partial v_p}{\partial x} + v_p \frac{\partial v_p}{\partial y} = \frac{1}{\tau} (v - v_p) \tag{6}$$

$$u_p \frac{\partial T_p}{\partial x} + v_p \frac{\partial T_p}{\partial y} = -\frac{1}{\gamma_T} (T_p - T) \tag{7}$$

where (u, v) and (u_p, v_p) are the velocity components of the fluid and dust particle phases along x and y directions respectively. μ, ρ_∞ and ρ_p are the coefficient of viscosity of the fluid, density of the fluid and mass of dust particles per unit volume of the fluid. T and T_p are the temperature of the fluid and temperature of the dust particle, c_p and c_s are specific heat of fluid and dust particles, γ_T is the temperature relaxation time, $\tau = 1/K$ is the relaxation time of the dust particle, K is the Stokes' resistances (drag coefficient). $\tau = 1/K$ is the thermal conductivity. In deriving these equations, the drag force is considered for interaction between the fluid and dust phases. The boundary conditions are

$$\begin{aligned} u &= U_w(x), \quad v = 0, \quad -k \frac{\partial T}{\partial y} = h_f(T_f - T) \quad \text{at } y = 0 \\ u &\rightarrow U(x), \quad u_p \rightarrow U(x), \quad v_p \rightarrow v, \quad \rho_p \rightarrow \rho\omega, \\ T &\rightarrow T_\infty, \quad T_p \rightarrow T_\infty, \quad \text{as } y \rightarrow \infty \end{aligned} \tag{8}$$

where $U_w(x) = bx$ is the stretching sheet velocity, $b > 0$ is stretching rate, ω is the density ratio, T_f is the hot fluid temperature and h_f is the heat transfer coefficient. By using the generalized Bernoulli's equation, in the free stream $U(x) = cx$ is simplified as

$$U \frac{dU}{dx} = -\frac{1}{\rho_\infty} \frac{dp}{dx} - \frac{\sigma B_0^2}{\rho_\infty} U. \tag{9}$$

Substituting (9) into (2) reduces to

$$\begin{aligned} u \frac{\partial u}{\partial x} + v \frac{\partial u}{\partial y} &= v \frac{\partial^2 u}{\partial y^2} + \frac{\rho_p}{\rho_\infty} (u_p - u) \\ &+ U \frac{dU}{dx} + \frac{\sigma_0 B_0^2 U}{\rho_\infty} (U - u) \end{aligned} \tag{10}$$

The mathematical analysis of the problem is simplified by introducing the following dimensionless coordinates in term of similarity variable and similarity function as

$$\begin{aligned} u &= bxf'(\eta), \quad v = -\sqrt{b}f(\eta), \quad \theta(\eta) = \frac{T - T_\infty}{T_f - T_\infty}, \\ \eta &= \sqrt{\frac{b}{\nu}}y, \quad \rho_r = H(\eta), \quad u_p = bxF(\eta), \\ v_p &= \sqrt{b}bG(\eta), \quad \theta_p(\eta) = \frac{T_p - T_\infty}{T_f - T_\infty}. \end{aligned} \tag{11}$$

By using the similarity equations from Equation (11), we obtain the following nonlinear ordinary differential equations:

$$\begin{aligned} f'''(\eta) + f(\eta)f''(\eta) - [f'(\eta)]^2 \\ + \beta H(\eta)[F(\eta) - f'(\eta)] + \lambda^2 + M(\lambda - f'(\eta)) = 0 \end{aligned} \tag{12}$$

$$\theta''(\eta) + \text{Pr}f(\eta)\theta'(\eta) + \frac{2\beta H(\eta)}{3}[\theta_p(\eta) - \theta(\eta)] = 0 \tag{13}$$

$$H(\eta)F(\eta) + H(\eta)G'(\eta) + H'(\eta)G(\eta) = 0 \tag{14}$$

$$G(\eta)F'(\eta) + [F(\eta)]^2 + \beta[F(\eta) - f'(\eta)] = 0 \tag{15}$$

$$G(\eta)G'(\eta) + \beta[f(\eta) + G(\eta)] = 0 \tag{16}$$

$$G(\eta)\theta'_p(\eta) + L_0\beta[\theta_p(\eta) - \theta(\eta)] = 0 \tag{17}$$

where $\rho_r = \rho_p/\rho_\infty$ is relative density, $\beta = 1/c\tau$ is the fluid particle interaction parameter, $M = \sigma B_0^2/\rho_\infty c$ is the magnetic parameter, $\lambda = c/b$ is the ratio of free stream velocity parameter to stretching sheet parameter, $\text{Pr} = \nu/\alpha$ is Prandtl number, $Bi = (\nu/b)^{1/2} h_f/k$ is the Biot number and $L_0 = \tau/\gamma T$ is the temperature relaxation parameter. The boundary equations in Equations (8) becomes

$$\begin{aligned} f(\eta) = 0, \quad f'(\eta) = 1, \quad \theta'(\eta) = -Bi(1 - \theta(\eta)) \quad \text{at } \eta = 0 \\ f'(\eta) \rightarrow \lambda, \quad F(\eta) \rightarrow \lambda, \quad G(\eta) \rightarrow -f(\eta), \quad H(\eta) \rightarrow \omega, \\ \theta(\eta) \rightarrow 0, \quad \theta_p(\eta) \rightarrow 0 \quad \text{as } \eta \rightarrow \infty. \end{aligned} \tag{18}$$

3.0 RESULTS AND DISCUSSION

The system of coupled nonlinear ordinary differential equations as in Equations (12) to (17) with boundary condition Equation (18) is solved by using RK45 method. The symbolic algebra software Maple is adopted given by Aziz [12] to solved these equations. Numerical solutions have been carried out to study the effect of various physical parameter such as ratio of free stream velocity parameter λ , fluid particle interaction parameter β , magnetic parameter M , Prandtl number Pr and Biot number Bi are shown graphically. In order to verify the accuracy of this study, Table 1 and Table 2 are drawn to compare the results obtained by Runge Kutta Fehlberg method. From Table 1, it is shown that the excellent agreement with reported by Hayat [13], Mahapatra and Gupta [14] and Ibrahim [15]. In Table 2, numerical values of local Nusselt number are compared with the existing solutions. Again, excellent agreement is seen between the solutions.

Table 1 Results validation for values of $f''(0)$ for existing solution for case $\beta = \omega = M = 0$ and $Bi = 1000$

| λ | Hayat [13] | Mahapatra and Gupta [14] | Ibrahim [15] | Present Result |
|-----------|------------|--------------------------|--------------|----------------|
| 0.01 | -0.9982 | -0.9980 | -0.9980 | -0.9981 |
| 0.1 | -0.9695 | -0.9694 | -0.9694 | -0.9694 |
| 0.2 | -0.9181 | -0.9181 | -0.9181 | -0.9181 |
| 0.5 | -0.6673 | -0.6673 | -0.6673 | -0.6673 |
| 2.0 | 2.0176 | 2.0175 | 2.0175 | 2.0175 |

Table 2 Results validation for values of $\theta'(0)$ for existing solution for case $\beta = \omega = M = 0$ and $Bi = 1000$

| Pr | λ | Hayat [13] | Mahapatra and Gupta [14] | Ibrahim [15] | Present Result |
|-----|-----------|------------|--------------------------|--------------|----------------|
| 1.0 | 0.1 | -0.6021 | -0.603 | -0.6022 | -0.6024 |
| | 0.3 | -0.6244 | -0.625 | -0.6255 | -0.6469 |
| | 0.5 | -0.6924 | -0.692 | -0.6924 | -0.6920 |
| 1.5 | 0.1 | -0.7768 | -0.777 | -0.7768 | -0.7764 |
| | 0.3 | -0.7971 | -0.797 | -0.7971 | -0.8184 |
| | 0.5 | -0.8647 | -0.863 | -0.8648 | -0.8640 |

In Figure 2, the characteristic of ratio of free stream velocity to the velocity of stretching sheet, λ on velocity profile with $Pr = 3, Bi = 10, \beta = 0.5, \omega = 0.02$ and $M = 1$ are shown. It can be observed that when free stream velocity is less than the velocity of stretching sheet, the velocity of the fluid and boundary layer thickness decreases. Otherwise, when free stream velocity is bigger than the velocity of stretching sheet, the velocity of the fluid increases while the boundary layer thickness decreases. While, when $\lambda = 1$, there is no boundary layer formation because stretching velocity is equal to the free stream velocity. Figure 3 shows the effect of ratio of free stream velocity to the velocity of stretching sheet λ on temperature profile. It is shown that the temperature decrease with the increase of λ .

The characteristic of fluid particle interaction β on velocity profile with $Pr = 3, Bi = 10, \omega = 0.02$ and $M = 1$ in the case when stretching sheet velocity is bigger than main stream velocity ($\lambda = 0.2$) are shown in Figure 4 whereas for the case when main stream velocity is bigger than stretching sheet velocity ($\lambda = 2.0$) are shown in Figure 5. These figures demonstrate that once the β increases, the fluid phase velocity decreases however the dust phase is increases. It is obvious from the figure that when the value of β become large, that is when the relaxation time decreases, then the velocities for both phases will be same.

Figure 6 illustrates the characteristic of M on velocity profile with $Pr = 3, Bi = 10, \omega = 0.02$ and $\beta = 0.5$ when $\lambda = 0.2$. It can be observed that the increase of magnetic number M when the velocity of stretching sheet is greater, the main stream velocity reduces the velocity of the fluid and dust phase. As M increase, the Lorentz force which opposes the flow also increases and decreases the velocity of the flow. While, in Figure 7 also shows the effect of magnetic parameter M on velocity profile in the case when velocity of the main stream is greater than the velocity of stretching sheet that is when $\lambda = 2.0$. Its shows that the increasing value of M , increase the velocity of the fluid and dust phase.

Effects of Prandtl number Pr on temperature profile with $\lambda = 0.2, Bi = 10, \beta = 0.5, \omega = 0.02$ and $M = 1$ for both fluid and dust phase are presented in Figure 8. We observed that the increasing number of Pr implies

the decreasing temperature of fluid and dust phase which implies the thicker momentum boundary layer than the thermal boundary layer. Figure 9 depicts the difference of Bi with $\lambda = 0.2, Pr = 3, \beta = 0.5, \omega = 0.02$ and $M = 1$ for the temperature profile of dust and fluid phase. The increasing of Biot number Bi increases the temperature profile for both fluid and dust phase.

Table 3 shows the velocity gradient $f''(0)$, wall temperature gradient $-\theta'(0)$ for a fixed values of $\lambda = 0.2$ and $\lambda = 2.0$. The effects of various physical parameters such as fluid particle interaction parameter, magnetic parameter, Biot number and Prandtl number are examined and discussed in detail. Examining the table, it reveals the increasing value of M , decreases the velocity gradient when $\lambda = 0.2$ but increases when $\lambda = 2.0$. Also, it can be observed that effect of increasing the value of β, Bi and Pr is to decrease the wall temperature gradient. While, the increasing value of Bi and Pr does not affect the velocity gradient for both case $\lambda = 0.2$ and $\lambda = 2.0$.

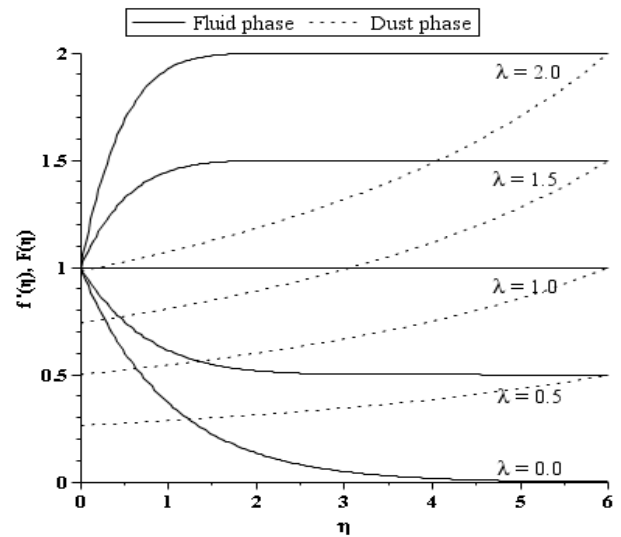


Figure 2 Velocity profiles for fluid phase $f'(\eta)$ and $F(\eta)$ dust phase for different values of λ

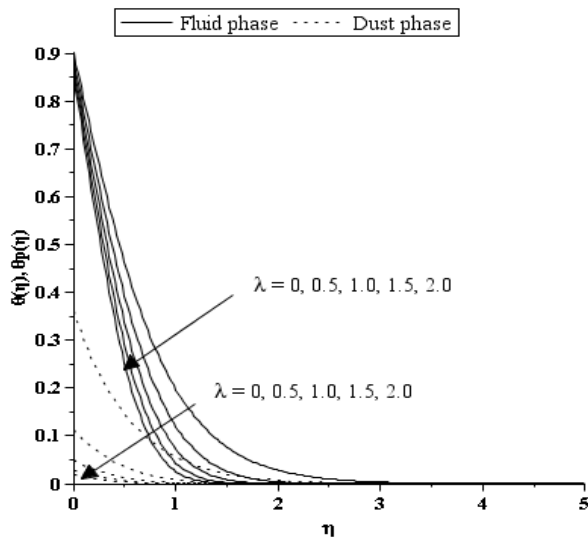


Figure 3 Temperature profiles for fluid phase $\theta(\eta)$ and $\theta(\eta)_p$ dust phase for different values of β

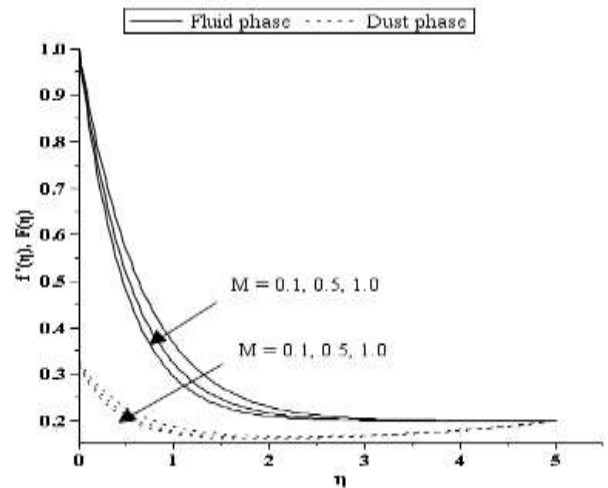


Figure 6 Velocity profiles for fluid phase $f'(\eta)$ and $F(\eta)$ dust phase for different values of M for $\lambda = 0.2$

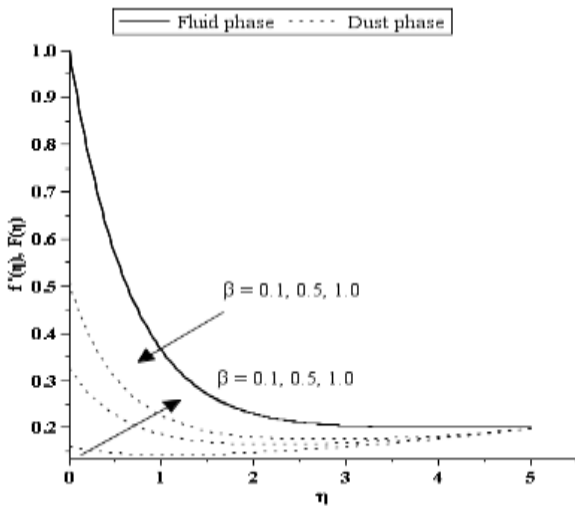


Figure 4 Velocity profiles for fluid phase $f'(\eta)$ and $F(\eta)$ dust phase for different values of β for $\lambda = 0.2$

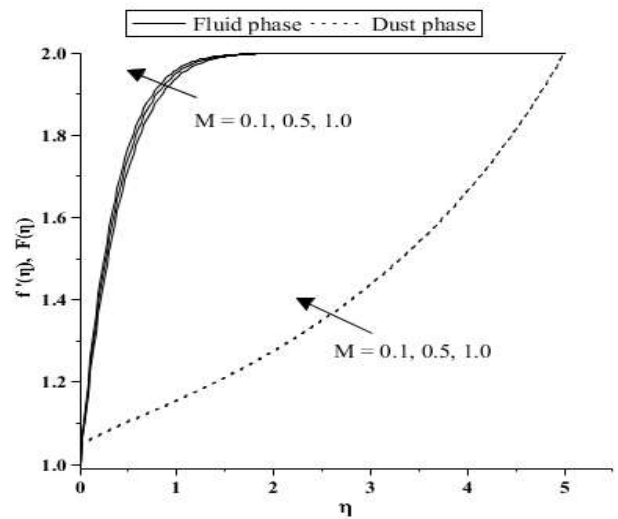


Figure 7 Velocity profiles for fluid phase $f'(\eta)$ and $F(\eta)$ dust phase for different values of M for $\lambda = 2$

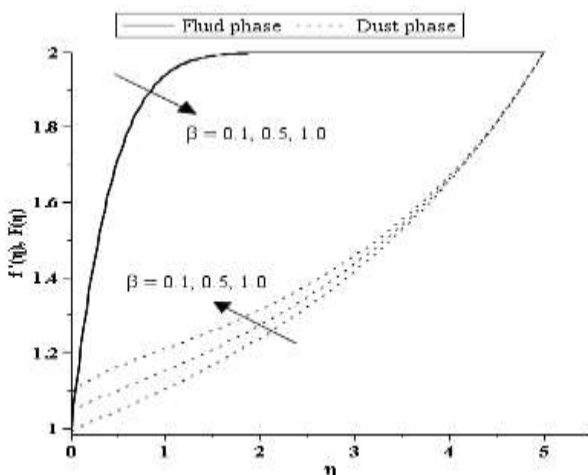


Figure 5 Velocity profiles for fluid phase $f'(\eta)$ and $F(\eta)$ dust phase for different values of β for $\lambda = 2$

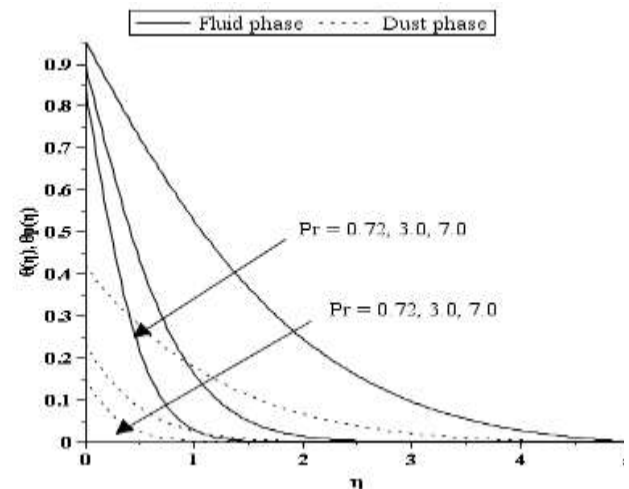


Figure 8 Temperature profiles for fluid phase $\theta(\eta)$ and $\theta(\eta)_p$ dust phase for different values of Pr

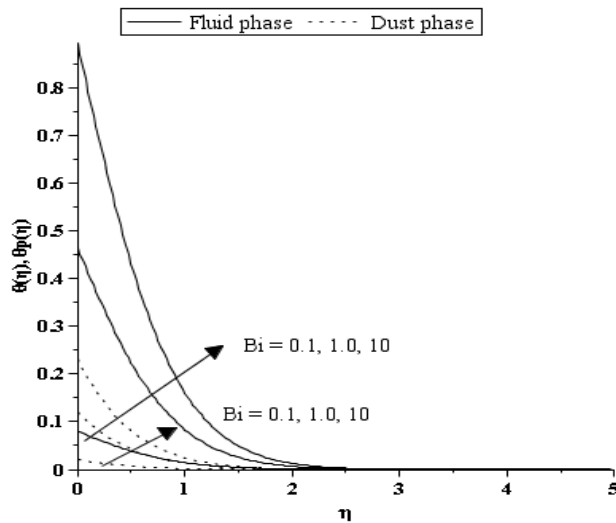


Figure 9 Temperature profiles for fluid phase $\theta(\eta)$ and $\theta(\eta)_p$ dust phase for different values of Bi

Table 3 Values of velocity gradient $f''(0)$ and wall temperature gradient $\theta'(0)$ for different β, M, Bi and Pr

| β | M | Bi | Pr | $\lambda = 0.2$ | | $\lambda = 2.0$ | |
|---------|-----|------|------|-----------------|---------------|-----------------|---------------|
| | | | | $-f''(0)$ | $-\theta'(0)$ | $f''(0)$ | $-\theta'(0)$ |
| 0.1 | 1 | 10 | 3 | 1.2160 | 1.0274 | 2.2488 | 1.4016 |
| 0.5 | | | | 1.2177 | 1.0284 | 2.2478 | 1.4021 |
| 1.0 | | | | 1.2195 | 1.0294 | 2.2466 | 1.4028 |
| 0.5 | 1 | 10 | 3 | 1.2177 | 1.0285 | 2.2478 | 1.4021 |
| | 2 | | | 1.4564 | 0.9991 | 2.4585 | 1.4101 |
| | 3 | | | 1.6614 | 0.9757 | 2.6529 | 1.4170 |
| 0.5 | 1 | 0.1 | 3 | 1.2177 | 0.0920 | 2.2478 | 0.0942 |
| | | 10 | | 1.2177 | 0.5341 | 2.2478 | 0.6199 |
| | | 100 | | 1.2177 | 1.0285 | 2.2478 | 1.4021 |
| 0.5 | 1 | 10 | 1 | 1.2177 | 0.4674 | 2.2478 | 0.7830 |
| | | | 2 | 1.2177 | 1.0285 | 2.2478 | 1.4021 |
| | | | 3 | 1.2177 | 1.5714 | 2.2478 | 1.9385 |

4.0 CONCLUSION

The analysis of stagnation point flow and heat transfer of a MHD dusty fluid with convective boundary condition over stretching sheet has been investigated. The effect of some parameters λ, β, M, Pr and Bi controlling the velocity and temperature profiles are shown graphically and discussed briefly. It is concluded that the effect of λ is to decrease the momentum boundary layer thickness. While, the effect of M is to decrease the momentum boundary layer thickness. It is interesting to note that the influence of β is to increase the velocity of dust phase but decrease the velocity of fluid phase. It is detected that the boundary layers are highly influenced by the

Prandtl number. The effect of Pr is to reduce the thermal boundary layer thickness. The effect of Biot number is to increase the thermal boundary layer.

Acknowledgement

The authors would like to thank for the support of the sponsors: Universiti Teknologi Malaysia for their financial funding through UTM Zamalah and MOHE for the financial support through vote 06H67, 4F255 and 4F538 for this research.

References

- (1) Saffman, P. G. 1962. On Stability Of A Laminar Flow Of A Dusty Gas. *J. Fluid Mechs.* 13: 120-128.
- (2) Chakrabarti, K. M. 1977. Note on Boundary Layer in a Dusty Gas. *AIAA J.*, 12: 1136-1137.
- (3) Vajravelu, K. and J. Nayfeh. 1992. Hydromagnetic Flow of a Dusty Fluid over a Stretching Sheet. *International Journal of Non-Linear Mechanics.* 27: 937-945.
- (4) Vajravelu, K., K. V. Prasad and P.S. Datti. 2013. Hydromagnetic Fluid Flow and Heat Transfer at a Stretching Sheet With Fluid-Particle Suspension and Variable Fluid Properties. *J. Fluids Engineering.* 135.
- (5) Rasekh, A., D. D. Ganji, S.Tavakoli, H. Ehsani and S. Naeefjee. 2014. MHD Flow and Heat Transfer of a Dusty Fluid Over a Stretching Hollow Cylinder with a Convective Boundary Condition. *Heat Transfer- Asian Research.* 43: 3.
- (6) Ramesh, G. K., B. J. Gireesha and Rama Subba Reddy Gorla. 2014. Boundary Layer Flow Past A Stretching Sheet With Fluid- Particle Suspension And Convective Boundary Condition. *Heat and Mass Transfer.*
- (7) Chiam, T. C. 1994. Stagnation-Point Flow Towards a Stretching Plate. *J. Phys. Soc. Jpn.* 63: 2443-2444.
- (8) Mahapatra, T. R. and A. S. Gupta. 2001. Magnetohydrodynamic Stagnation-Point Flow Towards A Stretching Sheet. *Acta Mechanica.* 152: 191 - 196.
- (9) Ramesh, G. K., B.J. Gireesha and C. S. Bagewadi. 2012. MHD Flow Of A Dusty Fluid Near The Stagnation Point Over A Permeable Stretching Sheet With Non-Uniform Source/Sink. *International Journal of Heat and Mass Transfer.* 55: 4900-4907.
- (10) Ramesh, G. K., B. J. Gireesha and C. S. Bagewadi. 2014. Stagnation Point Flow Of A MHD Dusty Fluid Towards A Stretching Sheet With Radiation. *Afr. Mat.* 25: 237-249.
- (11) Gireesha, B. J., G. M. Pavithra and C. S. Bagewadi. 2013. Thermal Radiation Effect on MHD Flow of A Dusty Fluid Over An Exponentially Stretching Sheet. *IJERT.* 2:2.
- (12) Aziz, A. 2009. A Similarity Solution for Laminar Thermal Boundary Layer over a Flat Plate with a Convective Surface Boundary Condition. *Communications in Nonlinear Science and Numerical.* 27: 1064-1068.
- (13) Mustafaa, M., T. Hayat, I. Pop, S. Asghar and S. Obaidat, 2011. Stagnation-Point Flow Of A Nanofluid Towards A Stretching Sheet. *Int. J. of Heat and Mass transfer.* 54: 5588-5594.
- (14) Mahapatra, T. R. and A. G. Gupta. 2002. Heat Transfer In Stagnation-Point Flow Towards A Stretching Sheet. *Heat and Mass Transfer.* 38: 517-521.
- (15) Ibrahim, W., B. Shankar and M. M. Nandeppanavar. 2013. MHD Stagnation Point Flow And Heat Transfer Due To Nanofluid Towards A Stretching Sheet. *Int. J. of Heat and Mass Transfer.* 56: 1-9.